Layered composite based on halloysite and natural polymers: a carrier for pH controlled release of drugs

Lorenzo Lisuzzo[a], Giuseppe Cavallaro[a,b], Stefana Milioto[a,b], Giuseppe Lazzara[a,b,*]

[a]Dipartimento di Fisica e Chimica, Università degli Studi di Palermo, Viale delle Scienze, pad. 17, 90128 Palermo, Italy. *giuseppe.lazzara@unipa.it*

[b]Consorzio Interuniversitario Nazionale per la Scienza e Tecnologia dei Materiali, INSTM, Via G. Giusti, 9, I-50121 Firenze, Italy

Abstract

We have prepared new biohybrid materials based on halloysite nanotubes and natural polymers (alginate and chitosan) for the controlled and sustained release of bioactive species. A functional nanoarchitecture has been designed allowing to generate a layered tablet with a chitosan/halloysite nanocomposite film sandwiched between two alginate layers. The assembly of the raw components and the final structure of the hybrid tablet have been highlighted by the morphological and wettability properties of the prepared materials.

Being that the biohybrid has been designed as a smart carrier, halloysite nanotubes have been firstly loaded with a model drug (sodium diclofenac). The effect of the tablet thickness on the drug release kinetics has been investigated confirming that the delivery capacity can be controlled by modifying the alginate amounts of the external layers. A simulation of the typical pH conditions along the human gastro-intestinal path has been carried out. Strong acidic conditions (pH = 3, typical in the stomach) prevent the drug release. In contrast, the drug has been released under pH = 5.7 and 7.8, which simulate duodenum/ileum and colon paths, respectively. These results demonstrate that the proposed nanoarchitecture is suitable as functional material with tunable delivery capacity.

Keywords: halloysite nanotubes; chitosan; alginate; biopolymer; drug delivery.

1. Introduction

Recently, the need to conciliate the technological progress with the growing environmental attention has become very compelling.[1] Hence, the design of new smart materials with sustainable characteristics was exploited for a wide range of applications.[2,3] Since the use of petrochemical-based plastic has to be restricted, bio-derived polymers represent a valid alternative for the preparation of new eco-friendly architectures.[4,5] Mostly, organic raw materials derive from agricultural or marine sources that can be functionalized in order to tune their main features such as the hydrophilic character, the thermal stability and the solubilization capability towards other compounds.[6–8] The biopolymers' charge is considered as a crucial point for their classification since they can be cationic (e.g. chitosan), anionic (e.g. pectin, alginate) or neutral species (e.g. amylose, starch and cellulose derivatives such as hydroxypropylcellulose) with consequent differences in their interaction behaviour and self assembly with other building blocks.[9–11] Biohybrid materials with variable structures and morphologies were successfully prepared by the assembly of natural polymers and inorganic particles.[12–14] Nowadays, these systems are attracting the attention of material scientists and engineers due to their wide applications including biomedical technology, catalysis, remediation, cultural heritage treatment and food packaging.[15–24] Recently, great efforts have been addressed to the design of biohybrid materials composed of organic moieties and inorganic clay minerals, which can present different features in terms of chemistry, aspect ratio, morphology and charge.[25,26] Among them, Halloysite Nanotubes (HNTs) are naturally occurring aluminosilicates composed by a layer of Si-O-Si tetrahedrons overlapped to Al-OH octahedrons that create a kaolinite-like sheet which further rolls up forming hollow tubular nanoparticles.[27,28] Halloysite dimensions strongly depend on its natural deposit. The HNTs external diameter is 50-200 nm, while the internal diameter and the lenght are 15-50 nm and 1-2 μm, respectively.[29,30] Besides their eco-sustainability and non-toxicity, their peculiar surface characteristics (different charge between the inner and outer surfaces due to their different Si/Al composition) make HNTs very interesting for charged guest molecules, which can be selectively adsorbed onto the nanotubes

through electrostactic and Van der Waals interactions.[31–34] Moreover, the tubular shape represents an appealing characteristic providing an encapsulation site for active molecules inside the lumen of the nanotubes, which can act as nanocarriers and delivery systems.[35–38] To this purpose, several smart materials have been prepared and exploited for the release of corrosion inhibitors, antiacid molecules, antioxidants and other species of biological interest such as antimicrobial agents and nonsteroidal anti-inflammatory drugs (NSAIDs).[39–47] In this regards, the selective functionalization of HNTs with stimuli responsive polymers (PNIPAAMs) allowed to create a new nanoarchitecture suitable for the drug release triggered by temperature.[48,49] Moreover, biohybrid gel beads composed by a chitosan embedded halloysite core in an outer alginate shell were prepared with the aim to enhance the control of the drug delivery.[50]

This paper contributes to the design of new smart biohybrid materials that can be used for health applications. Within this, halloysite nanotubes have been employed as both drug molecules nanocontainers and fillers for chitosan biopolymeric matrix. The coating of the nanocomposite film with alginate layers determined significant effects on the release kinetics as a function of the thickness of the layered tablets. More interestingly, the hybrid material was subjected to a simulation of the human gastro-intestinal path evidencing that strong acidic conditions (typical in stomach) prevented the drug release, which occurs under pH = 5.7 and 7.8 (simulating duodenum/ileum and colon, respectively). Therefore, the prepared hybrid tablet can be considered as an efficient system for a sustained and controlled drug delivery.

2. Results and discussion

2.1 Morphology and wettability of ALG/CHI-HNTs/ALG tablets

Table 1 lists the prepared layered tablets with variable alginate/chitosan-HNTs mass ratio ($R_{Alg/Film}$). The corresponding thicknesses of the interlayer film and the tablet are presented. It should be noted that both thicknesses were measured by a micrometer.

Table 1. Composition and thicknesses of the layered hybrid tablets

$R_{Alg/Film}$ (wt%)	CHI-HNTs thickness (μm)	Tablet thickness (mm)
20	58 ± 1	1.114 ± 0.001
25	44 ± 1	1.423 ± 0.001
30	60 ± 1	1.710 ± 0.001

The optical photographs of the tablet and details on cross sections of all the prepared samples are showed in Figure 1.

It is noteworthy the organization of the components in the ALG/CHI-HNTs/ALG hybrid materials (Figure 1 a,b,c). In particular, their structure is layered and the CHI-HNTs film is always visible within the cross section. The two alginate layers, covering the composite film on both its sides, present a homogeneous morphology and their dimensions strictly depend on the amount of biopolymer employed during the preparation phase. As expected, the $R_{Alg/Film}$ increase determined an enhancement of the tablet thickness (Table 1). All the three tablets have a sandwich-like structure, contrarily to the pure alginate tablet, which is reported for comparison in Figure 1d. As shown in Figure 1e, the nanotubes containing diclofenac are homogeneously dispersed within the chitosan matrix. This observation is promising for drug delivery purposes.

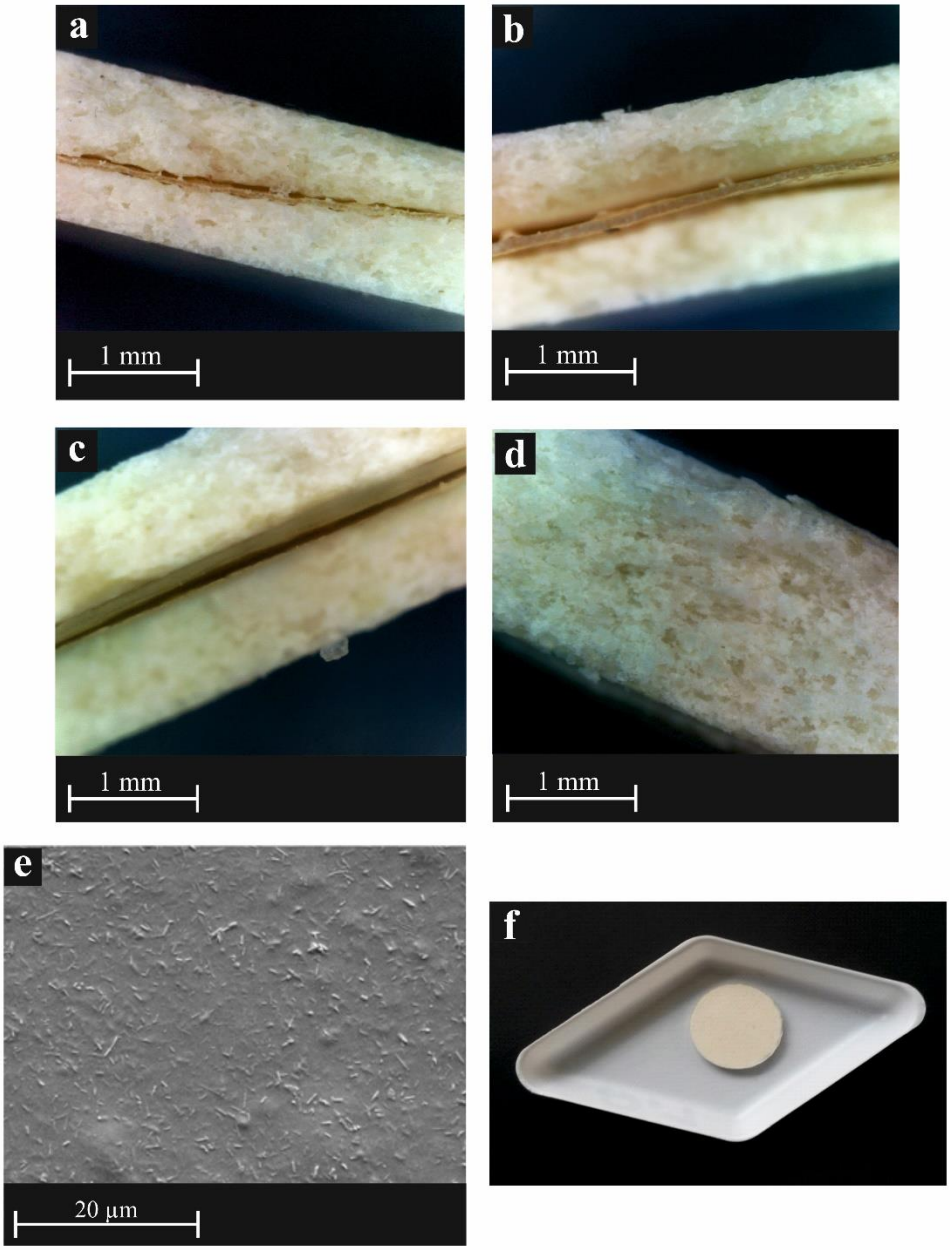

Figure 1. Cross section optical photographs of a) $R_{Alg/Film}$ = 20, b) $R_{Alg/Film}$ = 25, c) $R_{Alg/Film}$ = 30 and d) pure alginate prepared tablets; e) SEM image of the nanocomposite film based on chitosan and HNTs loaded with diclofenac; f) Optical photograph of the tablet with $R_{Alg/Film}$ = 20.

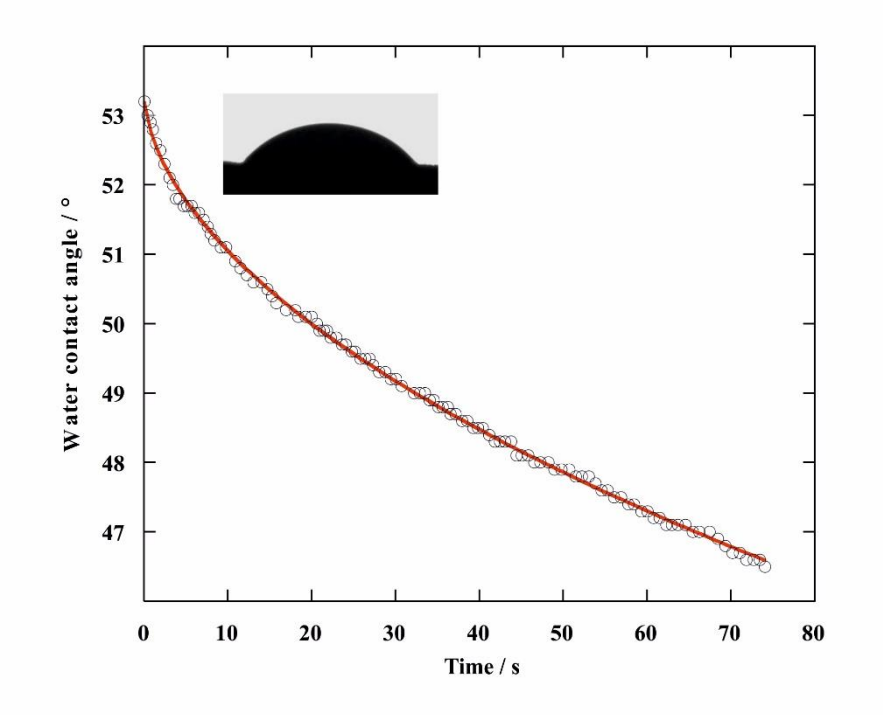

Figure 2. Water contact angle measurement as a function of time for $R_{Alg/Film}$ = 30 tablet. The inset displays the imaged of the water droplet just after surface deposition. The solid red line represents the fitting based on equation 2.

Contact angle measurements in water were carried out in order to study the wettability of the prepared materials. As an example, the θ vs t trend for the tablet with $R_{Alg/Film}$ = 30 is reported in Figure 2. The inset in Figure 2 displays the image of the water droplet just after its deposition onto the tablet surface. Table 2 reports the parameters resulting from the fitting the curves with equation 2.

Table 2. Wettability properties obtained the fitting of by θ vs t curves for tablet with variable composition.

Sample	θ_i (°)	k_θ	n
Alginate	59	0.0366	0.31
$R_{Alg/Film}$ = 20	64	0.1242	0.16
$R_{Alg/Film}$ = 25	58	0.0242	0.51
$R_{Alg/Film}$ = 30	53	0.0115	0.57

Errors: 1% for θ_i and k_θ,. 3% for n.

It was observed that all the tablets showed a hydrophilic character, since θ_i values are always lower than 90°. By comparing the results of the biohybrid materials with that of pure alginate tablet, it is noticeable that the specific sandwich-like structure and the thickness variation of the layers did not deeply alter the wettability degree. Moreover, the initial contact angle is always lower than that of chitosan/HNTs nanocomposite film, which was experimentally measured to be 79°, in agreement with literature.[51] As concerns k_θ, the hybrid tablets showed lower values compared to that of pristine alginate. Accordingly, we can state that the kinetics of the contact angle evolution was slowed down by the peculiar sandwich like structure of the hybrid tablets. Hence, *n* depends on both spreading and adsorption mechanisms. The n values ranged from 0.16 to 0.57 for $R_{Alg/Film}$ = 20 and $R_{Alg/Film}$ = 30, respectively. As a general result, we observed that the increase of the alginate amount in the hybrid systems determined an enhancement of the absorption contribution.

2.2 Release studies

The release kinetics of diclofenac from loaded HNTs, chitosan/HNTs nanocomposite film and ALG/CHI-HNTs/ALG tablets were investigated.

Preliminarly, we determined the amount of diclofenac encapsulated within the halloysite lumen by thermogravimetry. Figure 3 reports thermograms for pristine halloysite nanotubes, pure diclofenac and drug loaded HNTs. According to the rule of mixtures (see Supporting Informations),[52] we estimated a drug loading of 10.1 wt% by comparing the mass losses at 150 °C and the residual masses at 700 °C. This result is in good agreement with literature.[53]

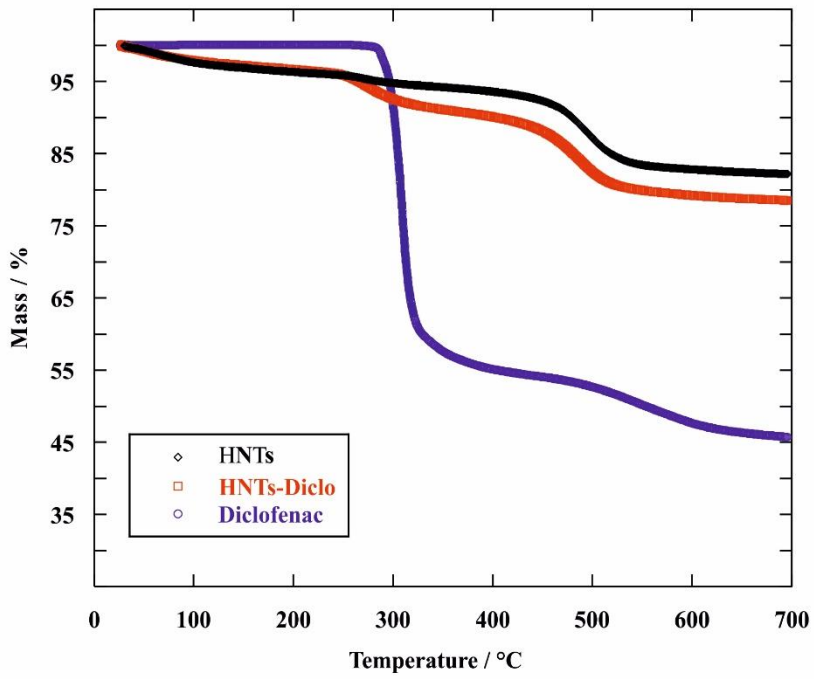

Figure 3. Thermogravimetric curves for HNTs, HNTs-Diclo and pure diclofenac.

2.2.1 Diclofenac release from loaded HNTs, chitosan/HNTs nanocomposite and layered tablets

Figure 4 compares the diclofenac release profiles for loaded HNTs and CHIT-HNTs nanocomposite film.

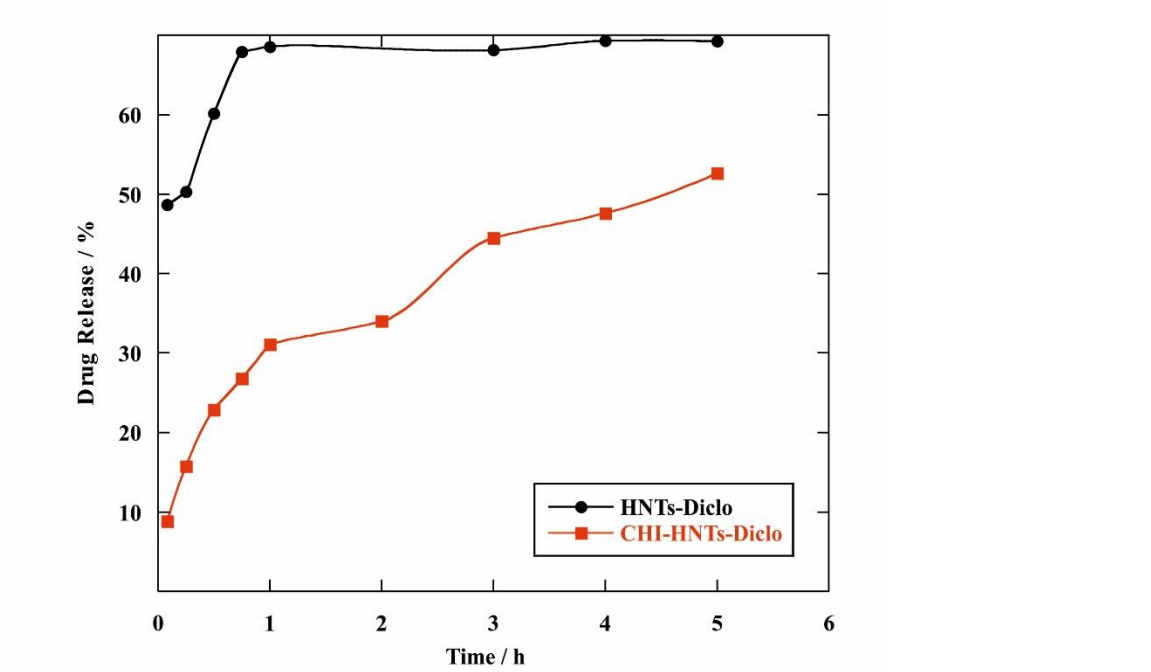

Figure 4. Release profiles for HNTs-Diclo powder and CHI-HNTs-Diclo nanocomposite film as a function of time.

It was observed that 48% of drug was released by the loaded clay nanotubes just after 5 minutes, while a saturation release (70%) was reached after 45 minutes. Compared to HNTs/Diclofenac, the release kinetics is slower for the drug loaded in the CHI-HNTs film. Specifically, we estimated that 9% and 52% of diclofenac is released after 5 min and 5 hours, respectively. This is most likely due to the barrier effect of the polymeric matrix, which can delay the drug release from HNTs inner lumen. Figure 5 reports the release kinetics for the biohybrid tablets with variable composition.

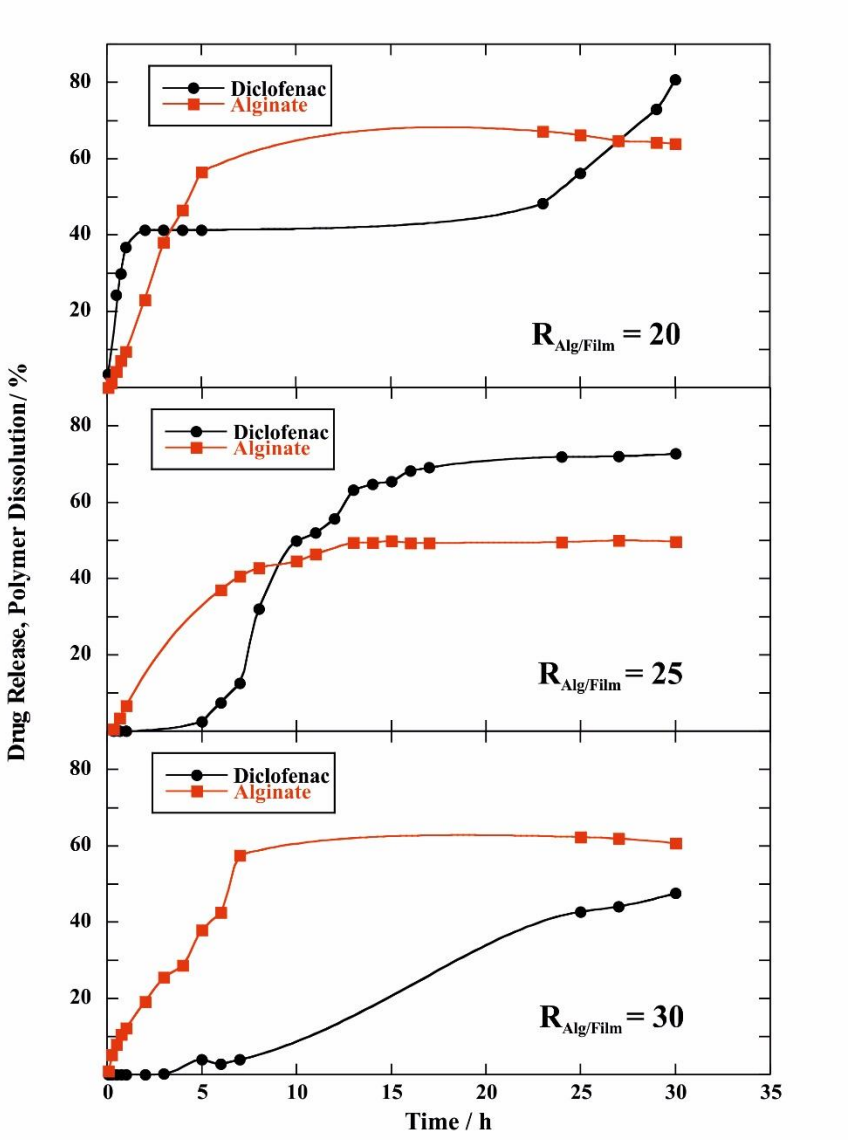

Figure 5. Release profiles for the three prepared tablets as a function of time.

As a general result, we observed that the presence of external alginate layers slows down the drug release kinetics. As concerns the hybrid with $R_{Alg/Film}$ = 20, we estimated that 3 and 40% of diclodenac are relased after 5 minutes and 2 hours, respectively. Interestingly, an interruption of the diclofenac release was observed after 2 hours, which corresponded to the starting time of the alginate dissolution in aqueous solvent. Once the alginate dissolution was complete (after ca. 5 hours), the drug release restated. Regarding the tablet with $R_{Alg/Film}$ = 25, an induction time of ca. 5

hours was observed for the diclofenac release process. The retardant effect on the drug release can be attributed to the protection of the external alginate layers of the hybrid tablet. Once the dissolved alginate concentration was constant (ca. 45%), the drug release exhibited an exponential increase reaching 50 and 70% after 10 and 24 hours, respectively.

Similar behaviour was observed for the tablet with $R_{Alg/Film}$ = 30, which showed a longer induction time (ca. 7 hours) for the diclofenac release. Only ca. 3% of drug was released during the polymer dissolution. Once the alginate concentration in the release medium was constant (ca. 57%), the drug was exponentially delivered reaching 42 and 47% after 24 and 30 hours, respectively.

To the light of these observations, we can state that the alginate layers played a relevant role in controlling the kinetics due to their swelling. We can hypothesize that the outer layers of alginate can absorb water from the medium causing the formation of a gel phase that delays the drug delivery. Once the biopolymer dissolution is complete, the diclofenac release from the hybrid is allowed. Remarkably, the different thickness of the ALG/CHI-HNTs/ALG tablets induced significant effects on the diclofenac release kinetics. In particular, the tablet with the thinnest alginate layers ($R_{Alg/Film}$ = 20) did not evidence a clear induction time for the drug release. In contrast, this effect was highlighted for tablets with a larger amount of alginate. Moreover, the total amount of diclofenac that could be released from the tablets was affected by the specific composition. In this regards, we estimated that the diclofenac release amounts after 30 hours are ca. 80, 65 and 45% for tablets with $R_{Alg/Film}$ = 20, 25 and 30, respectively.

2.2.2 Diclofenac release from the hybrid tablet under human gastro-intestinal conditions

Release studies from the hybrid tablet with $R_{Alg/Film}$ = 25 were carried out under different pH conditions simulating the human gastro-intestinal path. Specifically, the drug release kinetics were studied at pH = 3.0, 5.7 and 7.8, which simulate stomach, duodenum/ileum and colon paths. These tests were conducted at 37 °C in agreement with the human physiological conditions. Firstly, the tablet was kept in the aqueous solvent at pH = 3 for 2 hours. As shown in Figure 6, we observed a

negligible drug released amount (< 1%). Afterwards, the tablet was kept at pH = 5.7 for 1.5 hours. Here, we detected a jump on the diclofenac release up to ca. 5% (Figure 6). Lastly, the release medium was changed to pH = 7.8. We observed that the alkaline conditions favour the diclofenac release, which follows an exponential increasing trend (Figure 6). In particular, we estimated that the drug release are 12 and 75% after 4 and 50 hours, respectively. According to these results, we can conclude that the sandwich like structure of the hybrid tablet is efficient in controlling the drug release on dependence of the pH conditions of the phyisiological aqueous medium.

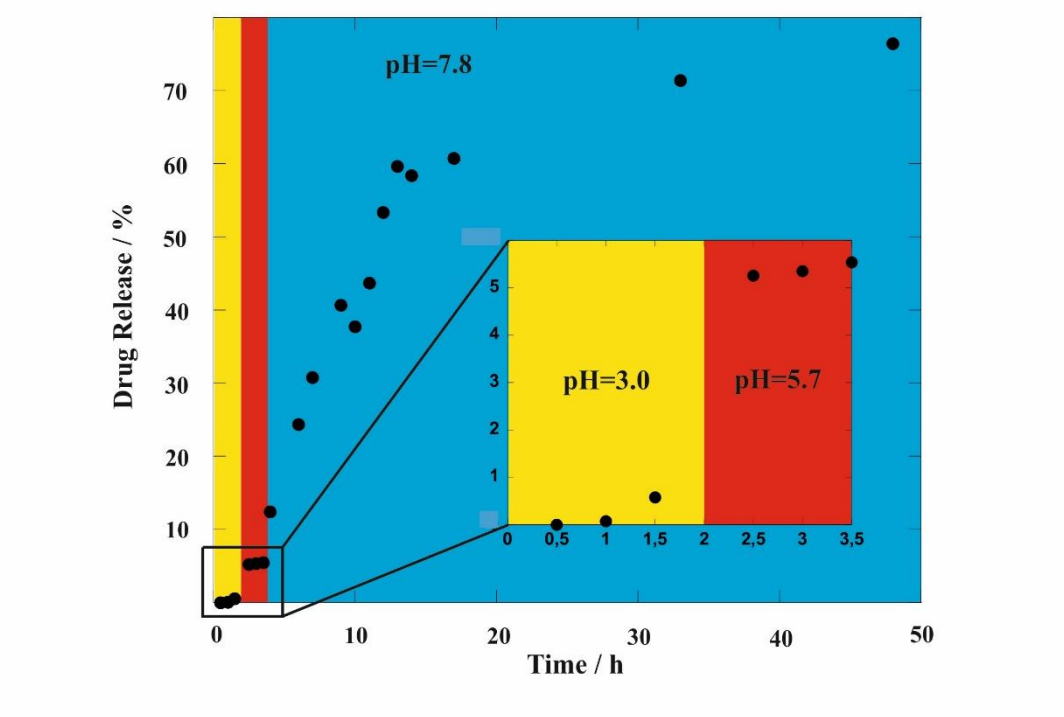

Figure 6. Release profile for the $R_{Alg/Film}$ = 25 tablet measured by simulating the human body gastrointestinal path most typical pH conditions, as a function of time.

3. Experimental section

3.1 Materials

Halloysite Nanotubes (HNTs) are a gift by Imerys Ceramics. Chitosan (Mw = 50–190 kg mol^{-1}), sodium alginate (Mw = 70–100 kg mol^{-1}), diclofenac sodium salt (Mw = 318.13 g mol^{-1}), acetic acid (≥ 99,5 %) , hydrochloric acid (37% v/v) and sodium hydroxide are Sigma Aldrich products.

3.2 Diclofenac loading of halloysite nanotubes

Accordingly to literature,[48] a diclofenac sodium salt saturated aqueous solution was prepared and HNTs powder was added in a 1:1 mass ratio. The dispersion was magnetically stirred for 24 h. Then, it was subjected to three vacuum cycles (P = 0.01 atm for 1 h) in order to optimize the loading efficiency.[52] It should be noted that the dispersion was stirred for 10 minutes between two consecutive vacuum cycles. Hence, the drug encapsulated nanoclay was separated by centrifugation (5 minutes at 8000 rpm) and it was washed with water and dried overnight in an oven.

3.3 Preparation of HNT-Chitosan-Alginate tablets

Firstly, a 2% w/w chitosan (CHI) solution in H_2O/acetic acid was prepared and halloysite loaded with diclofeneac was added at 0.6% w/w concentration. The dispersion was stirred for 24 h and it was poured into Petri dish in order to obtain CHI-HNTs nanocomposite films by solvent casting method. Afterwards, the film was cutted in several portions with a circular shape (diameter ca. 1 cm). The film was covered on both (top and bottom) sides with alginate (ALG) layers, which were compressed at 10 ton for 10 minutes allowing to generate a compact tablet (Figure 7). The amount of alginate was systematically changed endowing to prepare tablets with variable thickness.

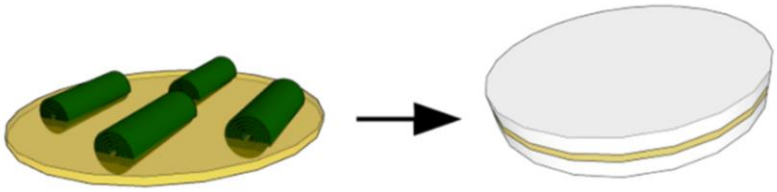

Figure 7. Schematic representation of the biohybrid tablet.

3.4 Diclofenac release kinetics

Release kinetics were studied by UV-VIS spectrophotometry. Hence, 10 mg of diclofenac loaded HNTs, 10 mg of CHI-HNTs film and the hybrid tablet with different thickness were placed into the release medium. At certain time intervals, 2 ml of liquid were taken from each sample, used for UV-VIS analysis and replaced with fresh solution. Release data were corrected using the following equation:[54]

$$C'n = Cn + \frac{V}{V_0} \cdot \sum_{i=0}^{n-1} Ci \qquad (1)$$

where Cn′ is the corrected concentration, Cn represented the nth concentration, V was the sample volume taken for each analysis (2ml), V_0 was the total volume.

In particular, kinetics were studied at pH = 7.8 for all the prepared systems. In addition, a simulation of the human body districts conditions was carried out by increasing pH from 3 to 5,7 to 7,8 (stomach, duodenum/ileum and colon, respectively).[55] Hence, since diclofenac and alginate have their main adsorption bands at $\lambda \approx 276$ nm, calibration curves were recorded for both the drug and the biopolymer in quartz cuvettes at the same acidic conditions.

3.5 Methods

Optical images were produced by using a DIGITUS® (DA-70351) microscope and processed by Digital Viewer software.

Water contact angle measurements were carried out by using an optical apparatus (OCA 20, Data Physics Instruments) equipped with a high-resolution CCD camera and a high-performance digitizing adapter. The water droplet was 10 ± 0.5 mL whereas gas phase was air and temperature was maintained at 25.0 ± 0.1°C. Data were acquired by SCA 20 software (Data Physics Instruments). Contact angle values on time were fitted by the following equation:[56]

$$\theta = \theta_i \cdot \exp(-k_\theta \cdot t^n) \quad (2)$$

where θ_i represents the initial value, k_θ and n are characteristic coefficients related to the process rate and mechanism. Specifically, n ranges between 0 and 1 on dependence of the absorption and spreading contributions to the kinetics, being 0 for the former and 1 for the latter, respectively.

Thermogravimetric analysis (TGA) was performed by a Q5000 IR apparatus (TA Instruments) under nitrogen flows of 25 cm^3 min^{-1} for the sample and 10 cm^3 min^{-1} for the balance, respectively. Thermal analysis was conducted on pure diclofenac, HNTs and diclofenac loaded halloysite by increasing the temperature to 700 °C with a scanning rate of 20 °C min^{-1}. The loading efficiency was provided through the rule of mixtures.[57]

UV-VIS spectrophotometer was used in order to study the release kinetics from the prepared materials. At this purpose, the employed equipment was a Specord S600 (Analytik, Jena, Germany).

A microscope ESEM FEI QUANTA 200F was used to image the halloysite nanotubes embedded into the Chitosan polymeric matrix. To this aim, the film was coated with gold in argon by means of an Edwards Sputter Coater S150A to avoid charging under electron beam. The measurements were conducted in high vacuum (< 6×10^{-4} Pa), while the energy of the beam and the working distance were set at 25 kV and 10 mm, respectively.

4. Conclusions

We prepared layered composite tablets based on biopolymers (alginate and chitosan) and halloysite nanotubes. The tablet fabrication consists of three steps: 1) loading of halloysite lumen with diclofenac as a model drug; 2) preparation of the nanocomposite film formed by chitosan and halloysite nanotubes containing diclofenac; 3) high pressure packing of the nanocomposite film between two alginate layers. Thermogravimetric experiments evidenced the successfull encapsulation (ca. 10.1 wt%) of the drug within the halloysite lumen, while Scanning Electon Microscopy showed that the loaded nanotubes were uniformly dispersed into the chitosan matrix. Optical observations of the hybrid tablets highlighted their peculiar layered structure with tunable thickness. The wettability properties of the tablets confirmed the sandwich like structure of the hybrids. The presence of the alginate layers slowed down the diclofenac release with respect to that from the nanocomposite film. In addition, we observed that the external biopolymer layers generated an induction time on the diclofenac release as a function of the tablet thickness. Similarly, the amount of drug released after a long time (30 hours) was affected by the composition of the hybrid tablet. These effects can be attributed to the protection of the alginate layers on the drug release. Interestingly, the sandwich like structure of the hybrid tablets allows to control the diclofenac release at variable physicological pH conditions. Under pH =3 (typical in stomach), the diclofenac release was negligible (< 1%), while an increase on the drug delivery was detected at pH = 5.7 (duodenum/ileum) being that the released amount was ca. 5%. Alkaline conditions (pH = 7.8, typical in colon) determined an exponential increase of the diclofenac release, which reachead 70% after 30 hours. Based on these results, we can conclude that the alginate/chitosan/HNTs hybrid is an effective and tunable delivery system that can be used for specific physiological purposes.

Conflicts of interest

There are no conflicts to declare.

Acknowledgements

The work was financially supported by Progetto di ricerca e sviluppo "AGM for CuHe" (ARS01_00697) and University of Palermo.

References

1 E. Forgacs, T. Cserháti and G. Oros, *Environ. Int.*, 2004, **30**, 953–971.
2 Y. Stetsyshyn, J. Zemla, O. Zolobko, K. Fornal, A. Budkowski, A. Kostruba, V. Donchak, K. Harhay, K. Awsiuk, J. Rysz, A. Bernasik and S. Voronov, *J. Colloid Interface Sci.*, 2012, **387**, 95–105.
3 T. Hueckel and S. Sacanna, *ACS Nano*, 2018, **12**, 3533–3540.
4 A. Takahara and Y. Higaki, *RSC Smart Mater.*, 2017, 131–156.
5 V. Bertolino, G. Cavallaro, G. Lazzara, S. Milioto and F. Parisi, *New J. Chem.*, 2018, **42**, 8384–8390.
6 A. C. S. Alcantara, P. Aranda, M. Darder and E. Ruiz-Hitzky, *J Mater Chem*, 2010, **20**, 9495–9504.
7 K. L. Hamner, C. M. Alexander, K. Coopersmith, D. Reishofer, C. Provenza and M. M. Maye, *ACS Nano*, 2013, **7**, 7011–7020.
8 F. Liu, L. Bai, H. Zhang, H. Song, L. Hu, Y. Wu and X. Ba, *ACS Appl. Mater. Interfaces*, 2017, **9**, 31626–31633.
9 V. Bertolino, G. Cavallaro, G. Lazzara, S. Milioto and F. Parisi, *Langmuir*, 2017, **33**, 3317–3323.
10 P. R. Chang, Y. Xie, D. Wu and X. Ma, *Carbohydr. Polym.*, 2011, **84**, 1426–1429.
11 E. A. Naumenko, I. D. Guryanov, R. Yendluri, Y. M. Lvov and R. F. Fakhrullin, *Nanoscale*, 2016, **8**, 7257–7271.
12 E. Ruiz-Hitzky, M. Darder, F. M. Fernandes, B. Wicklein, A. C. S. Alcântara and P. Aranda, *Prog. Polym. Sci.*, 2013, **38**, 1392–1414.
13 M. H. Shamsi and D. V. Geckeler, *Nanotechnology*, 2008, **19**, 075604.
14 M. Liu, R. Fakhrullin, A. Novikov, A. Panchal and Y. Lvov, *Macromol. Biosci.*, 2019, **19**, 1800419.
15 S. Sadjadi, T. Hosseinnejad, M. Malmir and M. M. Heravi, *New J. Chem.*, 2017, **41**, 13935–13951.
16 Y. Lvov and E. Abdullayev, *Prog Polym Sci*, 2013, **38**, 1690–1719.
17 R. F. Fakhrullin and Y. M. Lvov, *Nanomed.*, 2016, **11**, 2243–2246.
18 Y. Liu, H. Guan, J. Zhang, Y. Zhao, J.-H. Yang and B. Zhang, *Int. J. Hydrog. Energy*, 2018, **43**, 2754–2762.
19 C. Chao, H. Guan, J. Zhang, Y. Liu, Y. Zhao and B. Zhang, *Water Sci. Technol.*, 2018, **77**, 809–818.
20 G. Cavallaro, S. Milioto, F. Parisi and G. Lazzara, *ACS Appl. Mater. Interfaces*, 2018, **10**, 27355–27364.
21 G. Gorrasi, R. Pantani, M. Murariu and P. Dubois, *Macromol. Mater. Eng.*, 2014, **299**, 104–115.
22 C. Aguzzi, C. Viseras, P. Cerezo, I. Salcedo, R. Sánchez-Espejo and C. Valenzuela, *Colloids Surf. B Biointerfaces*, 2013, **105**, 75–80.
23 O. Owoseni, E. Nyankson, Y. Zhang, S. J. Adams, J. He, G. L. McPherson, A. Bose, R. B. Gupta and V. T. John, *Langmuir*, 2014, **30**, 13533–13541.

24 S. Sadjadi, M. Akbari, E. Monflier, M. M. Heravi and B. Leger, *New J. Chem.*, 2018, **42**, 15733–15742.
25 E. Abdullayev and Y. Lvov, *J. Mater. Chem. B*, 2013, **1**, 2894–2903.
26 C. Aulin, G. Salazar-Alvarez and T. Lindstrom, *Nanoscale*, 2012, **4**, 6622–6628.
27 Y. M. Lvov, D. G. Shchukin, H. Mohwald and R. R. Price, *ACS Nano*, 2008, **2**, 814–820.
28 Y. Joo, J. H. Sim, Y. Jeon, S. U. Lee and D. Sohn, *Chem. Commun.*, 2013, **49**, 4519–4521.
29 L. Lisuzzo, G. Cavallaro, F. Parisi, S. Milioto and G. Lazzara, *Ceram. Int.*, 2019, **45**, 2858–2865.
30 G. Cavallaro, L. Chiappisi, P. Pasbakhsh, M. Gradzielski and G. Lazzara, *Appl. Clay Sci.*, 2018, **160**, 71–80.
31 P. Pasbakhsh, G. J. Churchman and J. L. Keeling, *Appl. Clay Sci.*, 2013, **74**, 47–57.
32 Y. Zhang, Q. Liu, J. Xiang and R. L. Frost, *Appl. Clay Sci.*, 2014, **95**, 159–166.
33 V. Vinokurov, A. Stavitskaya, A. Glotov, A. Ostudin, M. Sosna, P. Gushchin, Y. Darrat and Y. Lvov, *J. Solid State Chem.*, 2018, **268**, 182–189.
34 B. Huang, M. Liu and C. Zhou, *Carbohydr. Polym.*, 2017, **175**, 689–698.
35 C. Aguzzi, P. Cerezo, C. Viseras and C. Caramella, *Appl. Clay Sci.*, 2007, **36**, 22–36.
36 T. G. Shutava, R. F. Fakhrullin and Y. M. Lvov, *Curr Opin Pharmacol*, 2014, **18**, 141–148.
37 S. Levis and P. Deasy, *Int J Pharm*, 2003, **253**, 145–157.
38 M. Du, B. Guo and D. Jia, *Polym. Int.*, 2010, **59**, 574–582.
39 G. Cavallaro, G. Lazzara, S. Milioto, F. Parisi, V. Evtugyn, E. Rozhina and R. Fakhrullin, *ACS Appl. Mater. Interfaces*, 2018, **10**, 8265–8273.
40 G. Gorrasi, *Carbohydr. Polym.*, 2015, **127**, 47–53.
41 E. Abdullayev and Y. Lvov, *J Mater Chem*, 2010, **20**, 6681–6687.
42 M. R. Dzamukova, E. A. Naumenko, Y. M. Lvov and R. F. Fakhrullin, *Sci. Rep.*, 2015, **5**, 10560.
43 A. Joshi, E. Abdullayev, A. Vasiliev, O. Volkova and Y. Lvov, *Langmuir*, 2013, **29**, 7439–7448.
44 H. Li, X. Zhu, H. Zhou and S. Zhong, *Colloids Surf. Physicochem. Eng. Asp.*, 2015, **487**, 154–161.
45 H. Zhang, C. Cheng, H. Song, L. Bai, Y. Cheng, X. Ba and Y. Wu, *Chem. Commun.*, 2019, **55**, 1040–1043.
46 J. Yang, Y. Wu, Y. Shen, C. Zhou, Y.-F. Li, R.-R. He and M. Liu, *ACS Appl. Mater. Interfaces*, 2016, **8**, 26578–26590.
47 K. Wang, Y. Zhang, J. Zhao, C. Yan, Y. Wei, M. Meng, X. Dai, C. Li and Y. Yan, *New J. Chem.*, 2018, **42**, 18084–18095.
48 G. Cavallaro, G. Lazzara, L. Lisuzzo, S. Milioto and F. Parisi, *Nanotechnology*, 2018, **29**, 325702.
49 D. N. Elumalai, J. Tully, Y. Lvov and P. A. Derosa, *J. Appl. Phys.*, 2016, **120**, 134311.
50 L. Lisuzzo, G. Cavallaro, F. Parisi, S. Milioto, R. Fakhrullin and G. Lazzara, *Coatings*, 2019, **9**, 70.
51 V. Bertolino, G. Cavallaro, G. Lazzara, M. Merli, S. Milioto, F. Parisi and L. Sciascia, *Ind. Eng. Chem. Res.*, 2016, **55**, 7373–7380.
52 L. Lisuzzo, G. Cavallaro, P. Pasbakhsh, S. Milioto and G. Lazzara, *J. Colloid Interface Sci.*, 2019, **547**, 361–369.
53 M. Makaremi, P. Pasbakhsh, G. Cavallaro, G. Lazzara, Y. K. Aw, S. M. Lee and S. Milioto, *ACS Appl. Mater. Interfaces*, 2017, **9**, 17476–17488.
54 D. Yu, J. Wang, W. Hu and R. Guo, *Mater. Des.*, 2017, **129**, 103–110.
55 J. M. DeSesso and C. F. Jacobson, *Food Chem. Toxicol. Int. J. Publ. Br. Ind. Biol. Res. Assoc.*, 2001, **39**, 209–228.
56 S. Farris, L. Introzzi, P. Biagioni, T. Holz, A. Schiraldi and L. Piergiovanni, *Langmuir*, 2011, **27**, 7563–7574.
57 M. Massaro, G. Cavallaro, C. G. Colletti, G. D'Azzo, S. Guernelli, G. Lazzara, S. Pieraccini and S. Riela, *J. Colloid Interface Sci.*, 2018, **524**, 156–164.